Electrolessly deposited diffusion barriers for microelectronics

by E. J. O'Sullivan

A. G. Schrott

M. Paunovic

C. J. Sambucetti

J. R. Marino

P. J. Bailey

S. Kaja

K. W. Semkow

Electrolessly deposited materials were investigated as possible diffusion barrier layers for multilayer microelectronic structures. Attention was focused on selective deposition of barrier layers on various surfaces, the barrier's capability to inhibit Cu diffusion, changes in Cu resistivity caused by barrier material diffusion into Cu, and adhesion between a polyimide film and the barrier layer. Electroless Co(P) was the most effective barrier to Cu diffusion at elevated temperature. even at Co(P) thicknesses as low as 500 Å. Diffusion-barrier effectiveness of electrolessly deposited materials decreased in the following order: $Co(P) > Ni-Co(P) \approx Ni(P) >> pure metals$ Co, Ni). Although a polyimide film bonded strongly to electrolessly deposited Ni(P) layers and only weakly to as-deposited Co(P), electroless Ni(P) significantly increased the Cu resistivity through interdiffusion. Polyimide adhesion to Co(P) was improved by oxidizing a Co(P) surface immediately after deposition to grow a passive film 50-75 Å thick, yielding a surface to which the polyimide adheres strongly and reproducibly. A low-energy-beam, scanning electron microscopy/energy-

dispersive X-ray analysis technique (SEM/EDX) was developed to measure the nonoxidized thin Co(P) barrier layer thickness.

Introduction

High-performance mainframe and midrange computers require a high density of interconnections, or "interconnects," for VLSI systems to take advantage of the fast speeds of integrated circuits available today. The interconnect systems normally consist of thin-film multilayers with conductor circuit planes and interlevel dielectric layers, the latter containing interconnecting vias. The dielectric may be a ceramic with conductor lines made of a refractory metal [1], or a polymer with copper conductors [2]. This paper discusses Cu–polyimide interconnect systems, although the conclusions reached are applicable to interconnect systems containing different polymer dielectrics.

In Figure 1, a schematic diagram is shown of a multilayer structure with layers of Cu interconnections embedded in polyimide [2]. Such a circuit structure is typically fabricated as follows: A blanket adhesion layer is applied to the surface of the substrate, which is, for example, a ceramic with its own circuitry or a silicon wafer. The first polyimide layer, one of whose functions is to planarize the substrate surface, is then applied. This is

©Copyright 1998 by International Business Machines Corporation. Copying in printed form for private use is permitted without payment of royalty provided that (1) each reproduction is done without alteration and (2) the Journal reference and IBM copyright notice are included on the first page. The title and abstract, but no other portions, of this paper may be copied or distributed royalty free without further permission by computer-based and other information-service systems. Permission to republish any other portion of this paper must be obtained from the Editor.

0018-8646/98/\$5.00 © 1998 IBM

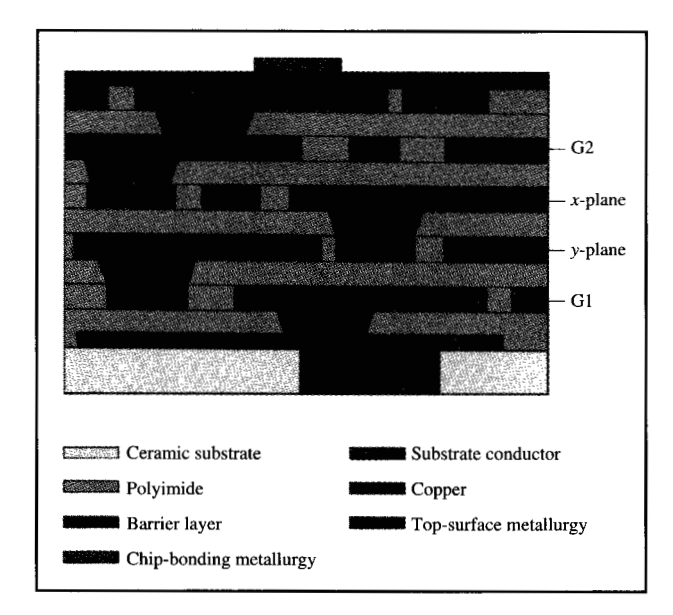


Figure 1

Schematic representation of a multilayer interconnect structure. G: ground plane.

followed by a layer of photosensitive polyimide, which is lithographically patterned to form trenches, e.g., 20 μm wide \times 10 μm deep. The first (underlying) polyimide layer is then etched to create vias to the top level of circuitry in the substrate.

An adhesion layer, such as Cr or Ta, and a Cu seed layer are blanket sputter-deposited onto the patterned polyimide. The Cu conductor thickness is built up through the two polyimide layers, either by further sputtering or by electrolytic or electroless deposition. The Cu layer is then planarized to the polyimide surface using a proprietary procedure. A barrier, or capping, layer is deposited onto the Cu for corrosion protection, for prevention of Cu interdiffusion with the next level of dielectric, and to ensure adhesion to the next polyimide layer.

A multilayer structure is formed by repeating the preceding process steps to form sequential polyimide layers with embedded Cu interconnections. After selective removal of polyimide to create vias, the exposed barrier layer at the bottoms of the latter is etched to reduce contact resistance prior to depositing a seed layer such as Cr/Cu. The final layer contains copper pads covered with suitable metals or alloys to enable chip bonding, e.g., using the C4 process [3]. Because of the temperature required for the C4 chip attachment process, and the need to fully cure the polyimide material, these multilayer package structures must withstand multiple processing cycles approaching 400°C, some of which may be up to one hour in duration.

The degradation of a Cu conductor in a multilayer structure by corrosion, poor adhesion, or interdiffusion is an important concern. Even in the absence of significant corrosion, a poorly passivating oxide layer present on Cu degrades adhesion at a polyimide/Cu conductor interface, especially under conditions of high-humidity and high-temperature processing of subsequent layers. Furthermore, as is discussed below, Cu dissolves into the interfacial region of the polyimide layer prior to curing, and adversely affects the dielectric and mechanical properties of the polymer to an unacceptable degree. Durable adhesion of polyimide to a Cu conductor is required for multilayers.

To prevent Cu corrosion and interdiffusion, a barrier layer is deposited on the Cu conductors prior to application of a layer of polyimide. An autocatalytic (electroless) deposition method for depositing a protective barrier layer on the exposed regions of the Cu conductors prior to polyimide spin-coating is described in this paper. The exposed Cu regions, which depend on the type of interconnect system fabricated, may be only the top surface of the conductors; the remaining surface regions of the Cu lines are protected by the sputtered adhesion layer deposited at the beginning of seed-layer formation. It is also possible to visualize a fabrication process whereby the sidewalls and top surface of the Cu conductors must be coated. A major advantage of an electroless barrier deposition process is that it is a selfaligning process that selectively clads the Cu conductors.

Also described in this paper are approaches for achieving adhesion of polyimide to an electroless barrier layer, and for measurement of barrier-layer thickness on individual conductors on an actual device substrate.

• Cu-corrosion reaction in the presence of polyamic acid (PAA)

The nature of the interactions between polyimides and various metal films has been investigated within IBM and elsewhere [4–7]. The interface formed by the evaporation, or sputtering, of metal films, typically adhesion-promoting layers, on *fully cured* polyimide, has been extensively studied [4, 5]. For an overlayer of polyimide on a metal, an uncured polyimide precursor, usually polyamic acid, is spin-coated onto the metal and then thermally cured.

Kim et al. [6, 7] studied the interface and adhesion of pyromellitic dianhydride-oxydianiline (PMDA-ODA) polyimide to several metals, including Cu and Cr. The polyamic acid form of PMDA-ODA was spin-coated onto metal films and then thermally cured to 400°C. From a cross-sectional, scanning transmission electron microscopy (STEM) study of the polyimide/Cu interface, they showed that very fine particles were present in the polyimide near the interface, and that these particles extended 6 μm up into thick (25-μm) polyimide layers. The particles were no

further than 100-200 nm from the polyimide/Cu interface. According to Kim et al. [6], this observation is due either to heterogeneous nucleation of the oxide particles or to a temperature and mobility gradient during curing that causes the interfacial Cu reaction product to migrate from the vitrifying polyimide into still plasticized polyamic acid. The larger-size particles were identified as Cu₂O by STEM and microdiffraction. Particles with a similar spatial distribution were also observed near the interface of cured polyimide/Ni structures [7], although fewer particles of NiO were observed compared to the Cu case. No particles were observed in similar polyimide/Cr structures. Kim et al. postulated that when polyamic acid (PAA) makes contact with Cu, the acid reacts with native oxide on Cu, forming a Cu(I)-PAA complex. During a cycloimidization step, CuOH forms and dehydrates to Cu₂O at the polyimide-curing temperatures, which may extend up to 400°C.

Cu dissolves in polyamic acid by dissolution of the thin native oxide normally present on Cu or after Cu oxidation by O_2 dissolved in the polyamic acid, thereby prolonging the Cu dissolution process until cycloimidization is complete.

Even when polyimide is deposited on Cu in a nonacid form and then cured, the polyimide/Cu interface may not be stable. If a significant oxide layer is present on Cu, the oxide does not possess the mechanical properties to survive thermal cycling and maintain the interface intact. An oxide-free Cu surface is virtually impossible to maintain in a manufacturing environment; also, polyimide does not form a sufficiently stable bond to Cu to withstand attack from trace amounts of O₂ in subsequent annealing steps, or when exposed to significant humidity. The relatively noble standard electrode potential (0.34 V vs. SHE¹) indicates that Cu does not possess the thermodynamic driving force to form a sufficiently stable passivating oxide layer that can bond strongly to polyimide when its precursor, polyamic acid, is used with adhesionpromoting coupling agents such as aminopropyl triethoxysilane (APS). In contrast, chromium forms an extremely stable thin oxide layer because of its low electrochemical series potential of $-0.74 \text{ V} (\text{Cr}^{3+}/\text{Cr}$ couple). The Cr oxide layer forms very stable bonds to polyimide via coupling agents such as APS.

• Barrier-layer considerations

Sputtered metal layers such as Cr, Ti, or Ta meet most technical requirements of an effective barrier for copper beneath a polymer. However, barrier-layer formation by sputtering is expensive and time-consuming, and it involves more than one processing step. The barriers are

Cr process		Electroless capping process	
Number of steps	Process	Number of steps	Process
i	Cr sputter	1 1	Pd catalyst
2	Resist spin	1 1	Electroless deposition
1	Resist expose	Total of 2-	-3 steps per layer
>1	Develop resist	 	
2	Cr sub-etch	! !	
>1	Resist removal	[[]	
Total of >8	steps per layer	ı	

Comparison of the number of processing steps involved in the sputtered Cr and electroless barrier processes.

first deposited as blanket films and then patterned and etched, followed by resist removal (Figure 2).

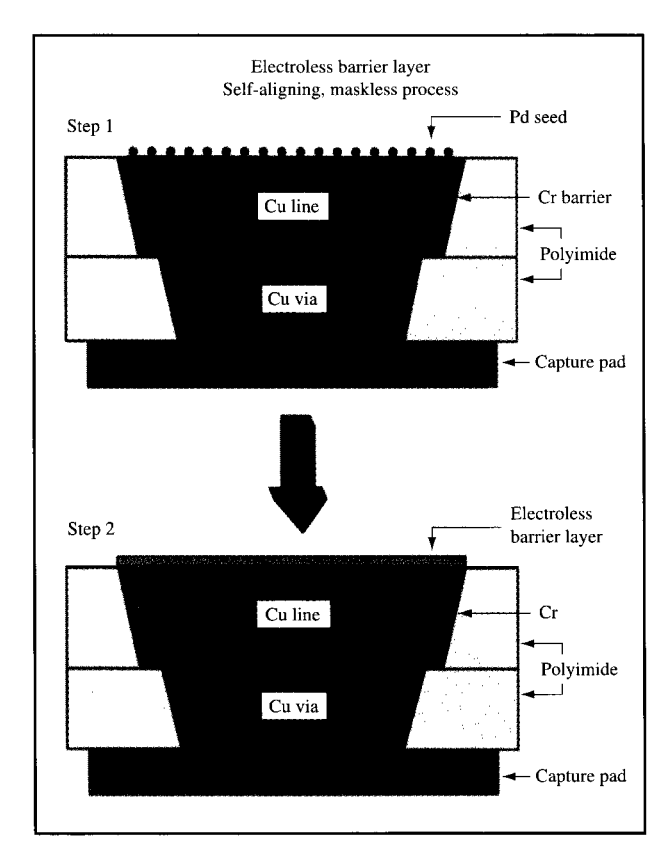
There is, therefore, considerable motivation to examine alternative materials for use as Cu diffusion barriers, such as those involving electroless deposition. Since an electroless process is self-aligning if properly carried out, patterning steps are not required after deposition. Figure 2 compares Cr metal-sputtering and electroless barrier-capping processes. The number of processing steps is considerably lower for the electroless barrier process.

Key objectives for the introduction of electroless systems in the interconnect packaging fabrication process are reduction of the number of process steps and improvement of the quality of the overall product with respect to a patterned barrier layer. Typically, some misalignment is expected, as for example in the lithographic patterning of the blanket-sputtered layers. Electroless Ni(P) and Co(P) are primarily investigated in the present study, these being well-known [8, 9] and relatively inexpensive processes.

• Some aspects of electroless deposition

Electroless deposition is a self-initiating, autocatalytic process in which a catalytically active surface is immersed in a solution containing complexed metal ions and a

SHE: standard hydrogen electrode.



Schematic representation of the Pd catalyzation and electroless deposition processes. Shown is a cross section of a conductor, line-via-capture pad feature.

reducing agent [8, 9]. The reducing agent converts the metal ions to zero-valent metal on the surface to form a continuous metal film. In the present case, hypophosphite was selected as the reducing agent. Because Cu is a poor catalyst for hypophosphite electrooxidation, a catalyst (usually a Pd-based one) must be applied to the Cu surface. This activation of the Cu surface with the Pd catalyst is termed *seeding*. The seeding step involves immersing the Cu surface in a dilute aqueous, acidic solution of palladium ions. A catalytically active layer of zero-valent Pd forms on the Cu surface through a chemical displacement deposition reaction (Figure 3).

A summary of the likely reactions involved in the electroless barrier deposition process involving hypophosphite as reducing agent is as follows for the Co case:

$$H_2PO_2^- \to (HPO_2^-)_{surf} + (H)_{surf}, \tag{1}$$

(2)

(3)

$$(HPO_2^-)_{surf} + OH^- \rightarrow H_2PO_3^- + e,$$

$$Co^{2+} + 2e \rightarrow Co$$
,

$$H_{2}PO_{2}^{-} + 2H^{+} + e \rightarrow P + 2H_{2}O_{2}$$
 (4)

$$(2H)_{\text{surf}} \to H_2. \tag{5}$$

 O_2 reduction may also occur on Cu/Pd and Co(P) surfaces:

$$O_2 + 4H^+ + 4e \rightarrow 4H_2O_2$$
 (6)

A key step is the dissociative adsorption of hypophosphite on the Pd seed catalyst and the Co(P) electroless layer [Equation (1)]. Strongly adsorbing solution stabilizers such as Pb2+ undergo competitive adsorption and influence the electroless deposition kinetics; to restrict the number of equations, they are not shown above. The hypophosphite adsorption and dissociation mechanism, which yields adsorbed atomic hydrogen and a hypophosphite radical anion, is similar to the generalized electroless deposition mechanism proposed by van den Meerakker [10]. In the above mechanism, reducing-agent dehydrogenation on the surface is the kinetic limiting step. Hypophosphite oxidation may not occur completely as discrete steps, as depicted in the above equations; instead, simultaneous adsorption and dissociation of hypophosphite may occur.

Equations (3) and (6) depict overall reactions, not reaction steps. It has not been determined whether the cobalt ion in Equation (3) is the hexaaquo complex or a citrate or citrate/borate complex. The reduction of dissolved O_2 is an important reaction in some electroless plating baths. Dissolved O_2 can significantly modify the induction time for electroless deposition by allowing time for deleterious side reactions, such as dissolution of the catalyst, to occur. On the other hand, dissolved O_2 ensures electroless solution stability by restricting the formation of Pd catalyst nuclei in the solution. Aided by the complexing power of the electroless solution, dissolved O_2 promotes dissolution of extraneous Pd seed nuclei present on the dielectric, thereby ensuring electroless deposition selectivity.

Phosphorus codeposition normally occurs in electroless nickel and cobalt solutions involving a hypophosphite reducing agent. Equation (4) represents a P deposition reaction. Although the recombination reaction for adsorbed atomic H is shown in Equation (5), some oxidation of H might also occur.

The phosphorus concentration present in the films from reaction (4) is dependent on pH (increasing at lower pH values) and on temperature and hypophosphite concentration. During film growth, coprecipitated phosphorus accumulates in the grain boundaries in the case of Co(P) deposits [8], while an amorphous phase is normally obtained in the case of Ni(P) for similar or larger P concentrations [8, 9]. The P imparts diffusion-

barrier properties to these binary alloys that are considerably different from those of the pure metals [11].

Results and discussion

A film (1000–2000 Å thick) of electroless Co(P) or electroless Ni(P) on copper prevents unwanted Cu dissolution reactions with the polyamic acid polyimide precursor. TEM characterization of the cured polyimide at the interfaces with these barrier materials showed no evidence of dissolution reactions between Co(P) and Ni(P) and polyamic acid. The barrier films were deposited using electroless solutions with rates of deposition of 150–300 Å/min. The rates of deposition of Ni(P) from these solutions are too rapid for good control of thickness, and possibly even for selectivity of deposition.

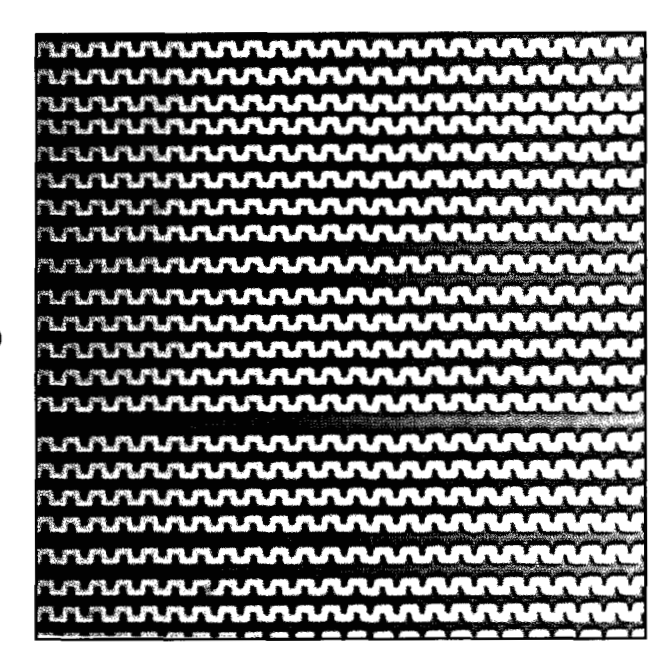
• Selectivity of deposition

A major requirement of the seeding operation is that of *selectivity*; i.e., the catalytically active palladium must be confined to the metal lines and completely absent from the adjacent polyimide surface [2]. Otherwise, the electroless solution would deposit barrier material onto areas of polyimide surface containing Pd, yielding shorts. The condition of selectivity is achieved by selection of the proper Pd compound [2] and by adjusting the parameters of the seed process, e.g., Pd²⁺ concentration and immersion time.

It is often necessary to follow the seeding step with a rinse solution containing a moderately strong complexant such as sodium citrate. Such a procedure yields excellent selectivity in the seeding and plating processes, with 100% coverage and no extraneous metal deposition between copper lines, provided that Co(P) and Ni(P) solutions are utilized that are properly maintained with respect to composition, pH, and concentration of dissolved O_2 . An example of an electroless Co(P) deposit on Cu conducting lines in this section of a circuit is shown in **Figure 4**. The Cu lines in this circuit have an interline spacing of $\sim 2~\mu m$ (narrower than the 5–15- μm spacing in typical packaging substrates) and a polyimide planarizing dielectric. The Cu conductors are covered with $\sim 1000~\text{Å}$ Co(P), which was deposited with excellent coverage and selectivity.

Diffusion-barrier properties

Since multilayer thin-film circuits containing high-temperature polymers such as polyimide may undergo many thermal cycles to 400°C, it must be established whether interdiffusion occurs in the Cu/barrier interfacial region at elevated temperatures. This was studied for films of electroless Co(P) and Ni(P), other metals such as electroplated Co and Ni, and evaporated Co, Ni, and Cr. Silicon-wafer (diameter 3.0 cm) test vehicles with the following structure were employed: Si/SiO₂/Cr/Cu/barrier film. The Cr adhesion layer was 400 Å thick and the Cu

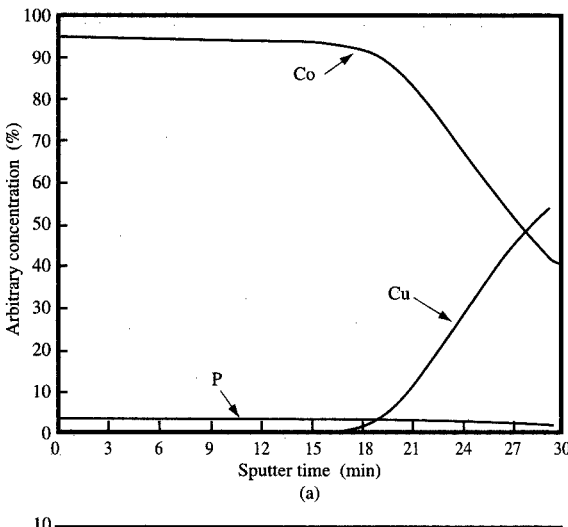


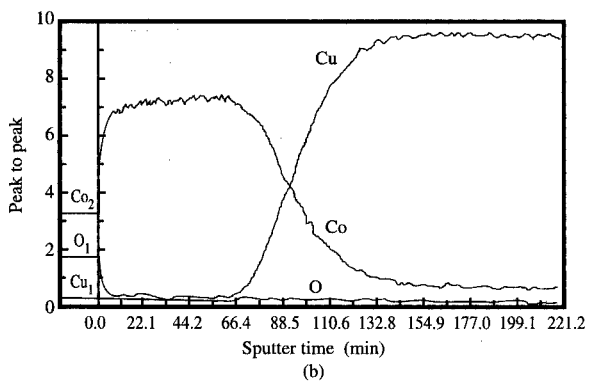
Portion of a circuit with 2000 Å electroless Co(P) on the Cu conductors. The smallest line spacing is 2 μ m.

4000 Å thick; both were evaporated. The thickness of the barrier films ranged from 500 to 2500 Å. The barrier films were annealed at 400°C in a forming gas (typically 95% $N_{\rm 2}$ + 5% $H_{\rm 2})$ atmosphere. After annealing, interdiffusion was characterized using Auger electron spectroscopy (AES) combined with sputter-profiling techniques.

Figures 5(a) and 5(b) show the AES profiles of 1200-Å-thick Co(P) films on Cu obtained before and after annealing the films for 14 hours at 400°C. A comparison of the profiles suggests that there is little if any intermixing of Cu and Co(P) after this extended heat treatment to 400°C. Shown in Table 1 is a comparison of AES depthprofile characterization results for Co(P), Ni(P), and Ni-Co(P) of various film thicknesses after annealing to 400°C for two hours. Significant concentrations of Cu were found in most of the barrier layers containing Ni. These results indicate that electroless Co(P) is a good barrier to Cu diffusion under the present processing conditions, but layers containing nickel are not. Substantially thicker Ni-Co(P) and Ni(P) layers prevent Cu diffusion, although the thinner layers are probably adequate with lowertemperature processing.

AES Cu depth profiles are shown in Figure 6(a) for evaporated Cr, Ni, and Co, and in Figure 6(b) for electroplated Ni, electroless Co(P), and Co(B). Copper diffusion is determined by measuring the copper concentration (at.%), which is shown as a function of





(a) AES depth profiles of Co, Cu, and P recorded for as-deposited, electroless Co(P) (1000 Å) on Cu. (b) AES depth profiles of Co, Cu, and O recorded for electroless Co(P) (1200 Å) on Cu after annealing to 400°C for 14 hours.

Table 1 AES depth-profile results for diffusion of Cu into Co(P), Ni(P), and Ni–Co(P) on Cu after annealing at 400°C for two hours.

Barrier	Cu in annealed barrier film (at.%)		
material thickness (Å)	Co(P)	Ni(P)	Ni–Co(P) alloy (50 at.% Co)
500	No Cu detected	1.3	1.0
1500	11	0.5	0.5
2000	11	0.2	0.1
2500	П	0.1	No Cu detected

sputter-removal time. It is apparent that the 500-Å-thick Cr film is a relatively poor diffusion barrier, probably owing to voids in the Cr film. However, a 1000-Å-thick Cr, similarly formed by evaporation, is a very effective diffusion barrier, although its use is impractical owing to the number of process steps required for its deposition and subsequent patterning. Figure 6(a) clearly shows that evaporated films of Ni and Co are very poor diffusion barriers: Copper concentrations greater than 20 at.% are present in these metals during initial sputter profiling. Likewise, electrodeposited films produced from either nickel sulfate or nickel sulfamate baths perform poorly as diffusion barriers [Figure 6(b)]. At the surface of the film derived from the nickel sulfate solution, the concentration of Cu is already about 30 at.%, and over 40 at.% for the nickel sulfamate solution film.

Figure 6(b) compares the behavior of electroless Co(P) and Co(B) films. In both cases the atomic percent of copper in the films is about zero even after 20 minutes of AES profiling (about halfway to the barrier-layer/Cu interface). In general, electroless Co(P) is more corrosionresistant than Co(B). The electroless solution used for electroless Co(P) is better understood, shows better selectivity, and is more stable with respect to extraneous deposition. Cobalt phosphorus is therefore more attractive as a barrier material than Co(B). At thicknesses of ~ 1000 Å, the electrodeposited thin films described tend to exhibit inferior diffusion barriers compared to electrolessly deposited materials. This is due to differences in film structures between the two classes of materials [11], principally to the presence of intermetallic phosphides in the electroless materials.

Table 2 shows the percentage of P typically found in electroless Co(P) layers for solutions containing different concentrations of citrate complexant. According to the phase diagram for this binary system [12], P exists in the form of Co₂P following heating to temperatures exceeding ~320°C. The phosphide intermetallic is thought to reside partly in the grain boundaries, where it exerts a blocking effect, restricting the diffusion of Cu through the Co(P) layer [11]. This mechanism is analogous to the so-called solute effect on inhibition of grain boundary and bulk diffusion [13-15]. A similar argument involving blocking of grain boundaries by intermetallic compounds formed on heating to ~350°C accounts for the good diffusion-barrier properties of Ni(P) and related electroless alloy films containing codeposited P. The reason for electroless Co(P) being a more effective barrier than electroless Ni(P) is not understood and requires further research. It may be related to factors such as grain size and distribution, and the nature of the respective phosphide intermetallics present in the grain boundaries.

The good diffusion-barrier properties of Cr films are probably due to the presence of chromium oxide in the

grain boundaries, which forms readily as a result of the large thermodynamic driving force for chromium oxide formation.

• Effect of electroless barrier layers on resistivity of copper To avoid increases in transmission delay, the resistivity of Cu in thin-film microelectronic structures must remain unchanged during processing. A typical criterion is that the capping process should not increase the Cu line resistivity by more than 3% (this corresponds to about 20 Å of Ni diffusing into $5 \mu m$ of copper, assuming all Ni goes into a homogeneous solid solution).

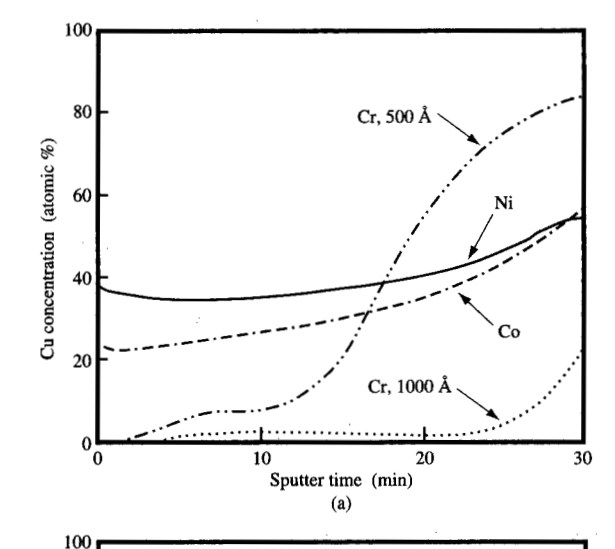
The variation of normalized resistivity obtained for 2-\$\mu\$m-thick Cu capped with 2000 Å Co(P) and Ni(P), which was heated to 400°C for various times, is plotted in Figure 7. For Ni(P) deposits, the Cu resistivity increased with time at 400°C, reaching 25% more than its initial value. No change was observed for Cu films covered with Co(P). This behavior is not surprising in view of the phase diagrams for the Cu-Co [16] and Cu-Ni [17] binary systems, which indicate that Ni and Cu are much more likely to intermix at temperatures of 300-400°C than Co and Cu. Despite its excellent corrosion-resistant properties, Ni(P) is not usable as a barrier material in thin-film circuits that are heated to 350°C or higher; electroless Co(P) is a more viable barrier material.

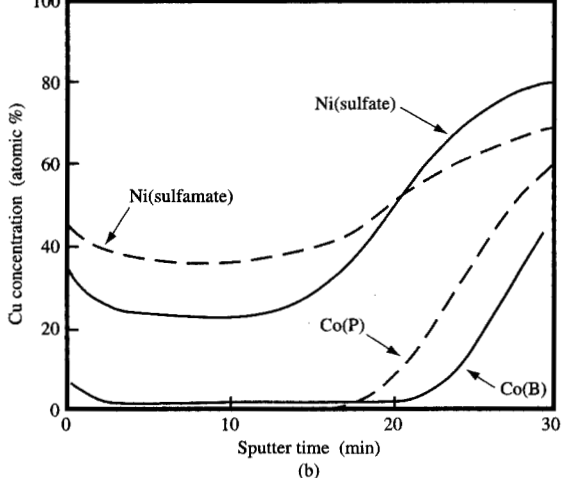
• Polyimide-barrier-film adhesion

An important function of barrier films is that they enable good adhesion between the dielectric, in this case biphenylene dianhydride-phenylenediamine (BPDA-PDA) polyimide, and the conductor line. Polyimide adhesion was characterized using the peel test method [18], with care taken to maintain the slowly peeling strip (2 mm wide) at a 90° angle to the substrate. The barrier films were spin-coated with aminopropyl triethoxysilane coupling agent prior to application of the polyimide films.

Electroless Ni(P) capping layers gave consistently good results for adhesion of BPDA-PDA to the Ni(P), with adhesion values equal to or even better than those obtained with Cr barriers in control experiments. In similar adhesion tests with electroless Co(P) barriers, the adhesion values were only marginal initially, and in many cases unacceptably low. The results for various barrier layers are summarized in **Table 3**. After peeling, cohesive failure was found in the polyimide for both Ni(P) and Cr capping layers. For Co(P), however, the mode of failure was delamination at the interface between the polyimide and the Co(P) surface, confirming that adhesion of polyimide to as-deposited Co(P) layers is intrinsically poor, even with an adhesion promoter.

Kaja et al. discovered [19] that adhesion on Co(P) was improved to about 50-70 g/mm by subjecting the Co(P) film to a mildly oxidizing ($\leq 2\%$ O₂ + H₂O) bake at



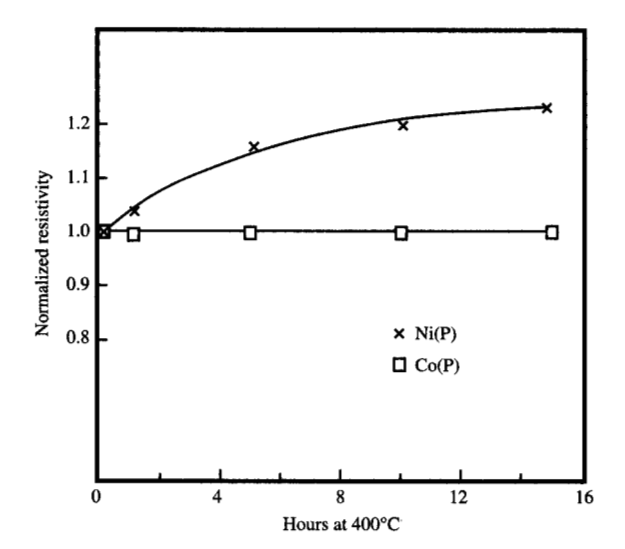


Floure :

(a) AES depth profiles of Cu recorded for evaporated Cr, Ni, and Co (1000 Å) films on Cu. Annealing conditions: 400°C for 14 h. (b) AES depth profiles of Cu recorded for electrodeposited Ni (1000 Å) and electroless Co(P) and Co(B) (both 1000 Å) films on Cu. Annealing conditions: 400°C for 14 h.

Table 2 Concentration of P in electroless Co(P) films deposited from solutions of different concentrations of citrate complexant. Other solution parameters included CoSO₄·7H₂O, 0.025 M; NaH₂PO₂·H₂O, 0.075 M; Pb(CH₃COO)₂, 1.15 µg/l; pH = 8.0; temperature = 73°C.

$Na_3C_6H_5O_7 \cdot 2H_2O$ (M)	P (at.%)
0.068	8.6
0.102	8.2
0.136	8.3
0.204	7.7
0.238	7.1



Finding.

Plot of normalized resistivity obtained for $2-\mu$ m-thick Cu films capped with 2000 Å Co(P) (\square) and Ni(P) (\times) that were heated to 400°C for various times.

Table 3 Summary of peel strength data for BPDA-PDA polyimide adhesion to a number of different barrier layers on Cu. Sputtered Cr thickness: 200 Å; electroless layers: 2000 Å.

Barrier material	Peel strength (g/mm)	
Cr	55-60	
Ni(P)	40-65	
Co(P)	5-45	

150-230°C to oxidize the surface. The characteristics of this passivating oxide layer, which is about 30-60 Å in thickness as determined by X-ray photoemission spectroscopy (XPS), are described below.

Thermally prepared Co(P) oxide films

Figure 8 shows the Co 2p XPS oxide peaks obtained after baking. Curve A shows a spectrum of the native oxide film. A similar spectrum is obtained if the sample is baked at 150° C for 30 min in a dry N_2 or N_2/O_2 mixture, prior to transfer to the analyzer chamber. The spectrum corresponds to a film ≈ 10 Å thick. In contrast, the spectrum of Curve B is observed after water vapor is added to the annealing gas mixture. The spectra are from oxide films ≥ 50 Å thick, and resemble Co_3O_4 in the width of the main peak and in the relative intensity of the

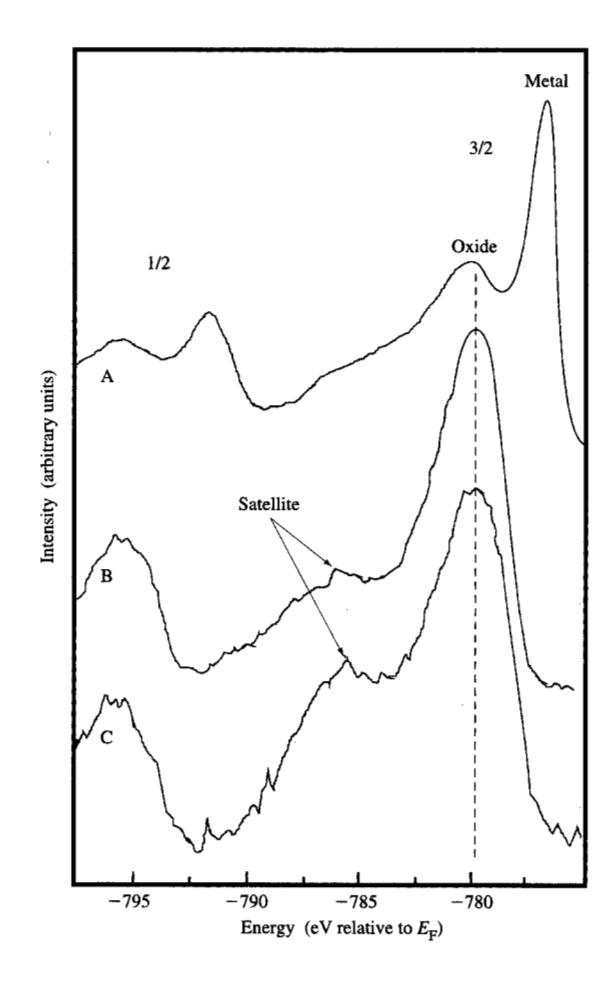


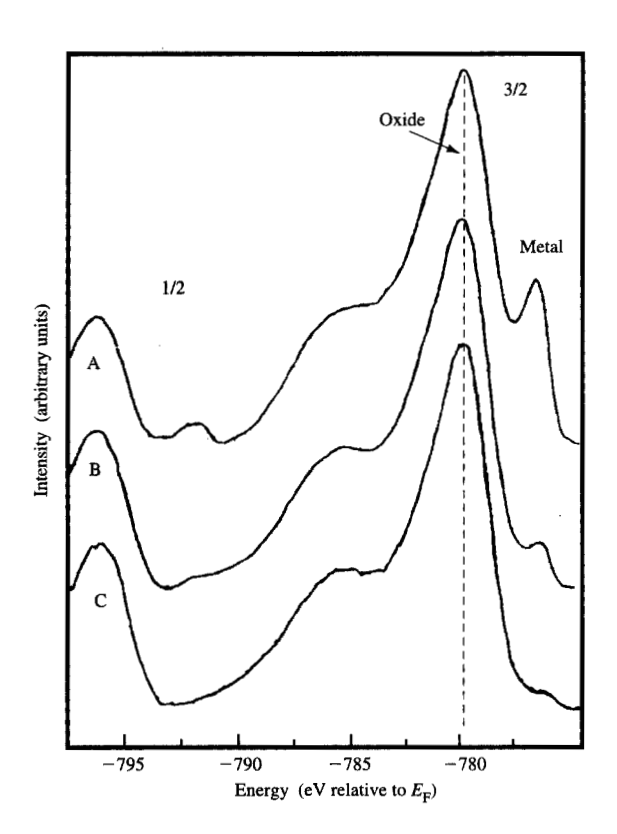
Figure 8

Cobalt 2p spectra for the following samples: Curve A, native oxide; Curve B, sample baked at 150°C in a N₂/O₂/H₂O mixture; Curve C, the sample of Curve B after 30 min at 300°C in vacuum.

satellite feature [20]. From the spectrum we infer the presence of both Co²⁺ and Co³⁺. The Co³⁺ concentration in these films is reduced by additional annealing in a reducing environment. Curve C is a spectrum corresponding to the sample of Curve B after an additional 30 min heating at 300°C in vacuum. Although this spectrum shows no metallic component, it exhibits a pronounced satellite intensity. These features are consistent with a CoO-like oxide film of similar thickness as before, produced during this reducing step.

Co(P) oxide films prepared in borate solution

The strong dependence of the Co oxidation on the content of H_2O in the baking atmosphere, and the need to control the O_2 , render the method impractical for manufacturing. Therefore, an immersion technique involving an aqueous





Cobalt 2p spectra for samples oxidized in a $B(OH)_3 + KOH$ solution at $60^{\circ}C$ for 5 min (Curve A), 10 min (Curve B), and 15 min (Curve C).

borate solution which grows the oxide film on the Co(P) layer immediately after electroless deposition and rinsing was developed. The concentration of O_2 from air dissolved in the borate solution was sufficient to grow the oxide at an acceptable rate. The O_2/OH^- couple in the borate anodically polarizes the Co(P), thereby driving the $H_2O/metal-oxide$ reaction. This method has the advantage of depending on controllable parameters such as time, pH, and bath temperature.

Figure 9 shows the Co 2p spectra for various Co oxide films obtained by immersion in a $B(OH)_3 + KOH$ bath of pH = 10 and at 60° C, for 5, 10, and 15 min. The oxide thickness obtained after 15 min (\approx 40 Å) yields acceptable (\approx 40 g/mm) peel strength values (see **Table 4**). A dependence on pH is shown in **Figure 10**, in which *valence-band* spectra for various oxides are obtained after immersion in a borate bath at 60° C for 15 min, with pH varying from 9.0 to 10.0. In addition to being more sensitive to the bonding state of Co than the 2p line, the valence spectra provide a better evaluation of the oxide

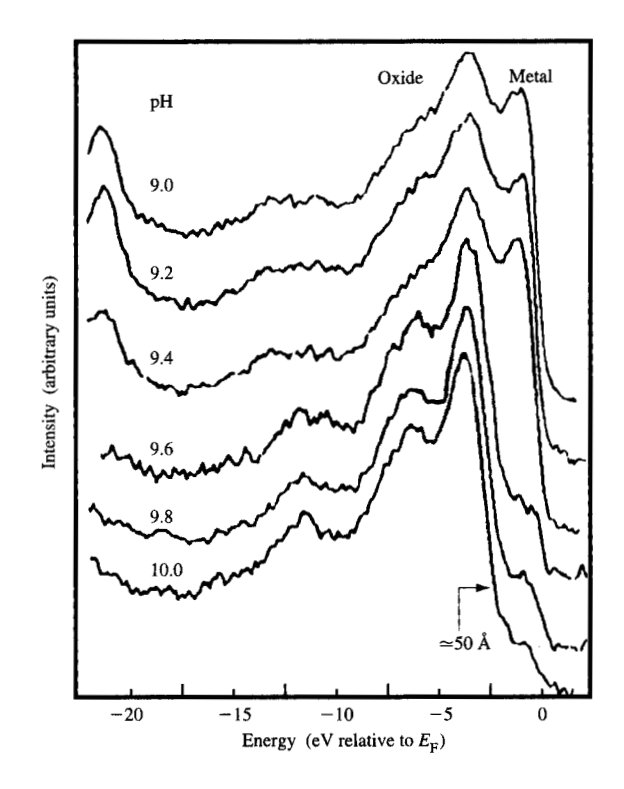


Figure 1.

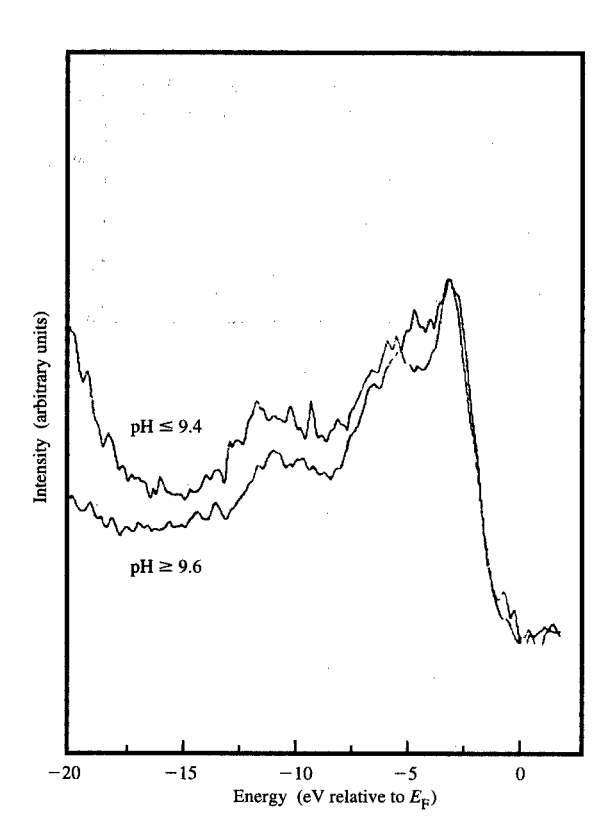
Valence-band spectra for samples immersed in B(OH)₃ + KOH solutions of increasing pH.

Table 4 Peel strength data obtained for BPDA-PDA polyimide adhesion to electroless Co(P) oxidized in borate solutions having different pH values. Borate concentration = 0.1 M; temperature = 60°C.

Borate solution	Peel strength	
(pH)	(g/mm)	
9.6-10.0	45–55	
9.0-9.4	20–40	

film thickness (50 to 60 Å) because of the higher kinetic energy (longer escape depth) of the valence photoelectrons [21]. The subtraction of the bare-metal signal is more easily accomplished using the valence spectra, since the intensity at the Fermi level arises only from the metallic component. Figure 10 illustrates a reproducible trend in the oxide thickness vs. pH. The thickness is estimated from the relative integrated intensities (areas under the peaks) of the signals from the Co metal and Co oxide, as compared to those films with





Valence-band spectra of Figure 10 for pH 9.4 and 9.6, after subtraction of the metallic component.

thicknesses larger than the escape depth. The estimation is performed by computing the following:

$$Z = \lambda \cos \theta \ln(R/R^* + 1)$$
,

where Z is the oxide film thickness and λ is the electron mean free path (25 Å); $R = I_{\text{Co ox}}/I_{\text{Co}}$ (I_{Co} and $I_{\text{Co ox}}$ refer to signal intensities of oxide-free and oxide-covered Co, respectively); R^{\times} is the signal ratio for oxide and metal films (measured separately) thicker than the escape depth (\sim 80 Å); and θ is the electron take-off angle. The estimated thickness ranged from \approx 20 Å for pH = 9.0 to \approx 50 Å for pH = 10. Oxides grown at a fixed pH at higher temperatures increase in thickness. The selection of pH and temperature is based upon practical considerations.

The trend in peel strengths shows routinely good values for $pH \ge 9.6$ (see Table 4). Figure 10 shows a pronounced change in the oxide thickness on going from pH = 9.4 to pH = 9.6. This suggests that passive oxide film formation is important for good adhesion, and because it prevents the interaction of the polyamic acid with Co, thus

inhibiting the formation of unwanted phases at the interface. In addition, the oxide films grown at $pH \ge 9.6$ seem to exhibit a different chemistry than those grown at $pH \le 9.4$; this may also play a role in the adhesion of the polyimide to the oxide, as is discussed later. The difference in chemistry is more clearly appreciated in **Figure 11**, which shows the Co 2p spectra for the samples corresponding to pH = 9.4 and 9.6, after subtraction of the metallic component. The samples grown at $pH \le 9.4$ show a broader shoulder, which indicates a larger concentration of Co^{2+} in the oxide [22] compared to that of $pH \ge 9.6$. Similar information is obtained from the Co 2p core-level spectra.

XPS analyses of both the substrate and the back of the polyimide after a peel test offer additional support for the role of the surface chemistry in enhancing the adhesion of the polyimide to the oxide. To understand the following results, one should keep in mind that a Si-based adhesion promoter is spun onto the substrate prior to the deposition of the polyamic acid.

The XPS spectra for the back of the peeled PI showed the following features: Co oxide was detected, as well as a significant amount of Si (relative large Si-to-N peak-area ratio) in the PI peeled with low peel strength. In contrast, for the high-peel-strength samples, the Si-to-N intensity ratio was low, and no Co oxide was detected. The presence of Co oxide in the former suggests a fracture path running through the oxide. This is expected for a thin, nonpassivating film. The high concentration of Si in the polymer suggests a weak Si/oxide bond. Conversely, for the high-peel-strength sample, the lower Si-to-N ratio should imply a stronger Si/oxide bond. This is corroborated by the spectra from the peeled substrate. The Co³⁺-richer substrate that corresponds to the high-peel-strength sample exhibits a higher Si-to-Co ratio.

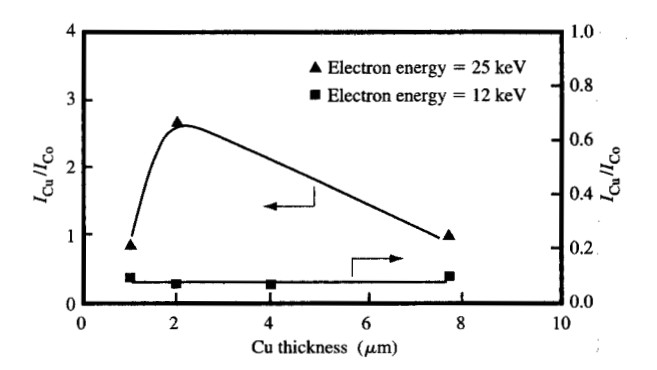
Our results strongly indicate that an oxide layer $\approx 50 \text{ Å}$ thick is required for acceptable adhesion of polyimide because it provides a passivating film that prevents reaction of the polyamic acid with Co. However, a film grown too thick may lose its passivating properties because of stress-induced effects. As for the effect of the surface chemistry, it can be understood in terms of the local electronic structure for Co oxides derived from cluster calculations [22, 23]. CoO contains Co²⁺ ions in octahedral sites, with configuration $t_{2g}^5 e_g^2$. In Co_3O_4 , Co^{2+} ions with $t_{2g}^3 e_g^4$ configuration occupy tetrahedral sites, and Co^{3+} ions with t_{2g}^{6} configuration occupy octahedral sites. The atomic arrangement at the octahedral sites in the spinel structure of Co₂O₄ exhibits sites [24] which may be suitable for a strong bond to the Si in the adhesion promoter. Appropriate atomic distances and electronic configuration are both favorable for a strong interaction with the silica tetrahedra. The O-O bond length in Co₂O₄ is ≈ 2.8 Å, which is similar to the atomic distances in the

base of a tetrahedron formed by Si in many compounds [25]. Therefore, it seems to be a good geometrical match between the base of the tetrahedra and the atomic arrangement at the surface. Thus, at least two of the oxygens of the silica tetrahedron could be replaced by O of the surface lattice, maintaining the O-Si-O angle within the interval 108-110° that is representative of most Si compounds [25]. On the other hand, in Co₃O₄ there are more electrons in the t_{2g} configuration than in CoO. These orbitals do not hybridize with the O 2p orbitals of the O near neighbors, and do not form σ bonds but point diagonally toward the second nearest neighbors to form π bonds. The latter lie at higher energy, favoring rehybridization in the presence of Si in comparison to σ bonds. In contrast, CoO has a NaCl structure, with a Co-Co(O-O) distance of ≈ 3 Å, which matches poorly with the O-O distance in the Si tetrahedra. In addition, the Co²⁺ ions have electronic configurations that make σ bonds predominant [23]. Thus, we expect a weaker Si-surface bond on CoO.

The above explanation is consistent with the variation in Si content for the substrate and polyimide side of the peeled samples measured in our XPS experiments. We have established a good correlation between the presence of a thin oxide layer on Co(P) containing Co^{3+} ions and acceptable adhesion of PI to Co(P). We have shown that a Co_3O_4 -like oxide film ≈ 50 Å thick produces a passive layer, as well as the appropriate surface chemistry for interaction with the Si-based adhesion promoter. We have identified a suitable oxidation method, as well as the parameter window that yields the best interfacial properties.

The advantages of the solution oxidation process are simplicity, low cost, and rapid passivation of the Co(P). The conditions for formation of the oxide are as follows: After the deposition of the Co(P) layer, the sample is rinsed and immersed in a solution of 0.1 M H₃BO₃, at a pH of 9.5–10 and a temperature of 55–60°C. The solution has dissolved oxygen in equilibrium with air, and requires an immersion time of less than 10 minutes.

• A new thickness measurement technique for electroless films. Formation of the barrier layer is just one of many steps in the process of building a multilayer package, and the requirements of the overall process impose a narrow window on the thickness of the electrolessly plated barrier film. Because of the complicated nature of the electroless deposition process, which is influenced by so many variables (e.g., the additives and dissolved O₂), the thickness of the plated layer may depend among other things on feature size. Therefore, a thickness calibration derived from measurements carried out on blanket parts may not be sufficiently reliable to characterize deposit thickness on features of different sizes.



Cu/Co K α intensity ratio for a 2500-Å Co(P) film plated onto Cu substrates of different thicknesses. Triangles: 25-keV beam energy; squares: 12-keV beam energy.

Because of its good lateral resolution, we have used a low-energy-beam SEM/Energy Dispersive X-ray (SEM/EDX) analysis technique to characterize the thin capping barrier layers. Figure 12 (triangles) shows the Cu/Co Kα ratios of a 2500-Å Co(P) layer plated onto Cu underlayers of different thicknesses, measured by EDX using a 25-keV electron energy. The variations from sample to sample underscore the potential problems in trying to use this electron energy to measure the thickness of the Co layer. In contrast, also shown in Figure 12 (squares) is a similar measurement performed with a 12-keV electron energy. In this case, the values do not vary significantly from the Cu thickness. Since in real packaging parts the minimum Cu thickness is greater than 2 μ m, the effective volume of interaction is always included in the Cu layer, and the emitted radiation should not reflect variations in the thickness of Cu. It is apparent from the calculations in Figure 13 of effective volumes for X-ray generation by the electron beam for different electron energies that a lower-energy electron beam is required.

The standard operation of an SEM usually involves incident electron energies of ~ 25 keV. The effective region is then of the order of that defined by the thickness of the Cu underlayer in a packaging array. Thus, variations in the Cu thickness may result not only in variations of the Cu K α intensity, but also in variations in the Co K α due to second-order effects. This would be detrimental to the use of the SEM/EDX for the measurements of interest, because the underlying thickness of Cu varies from feature to feature. A lower-electron-energy beam generates a smaller interaction volume, as shown in Figure 13. The Co/Cu K α ratio should reflect only variations in the thickness of the plated

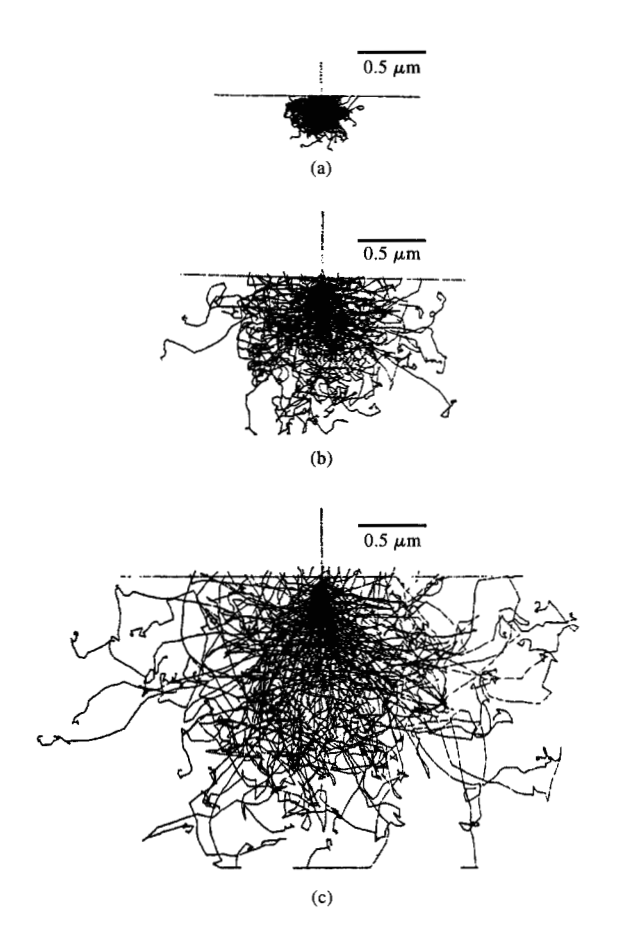


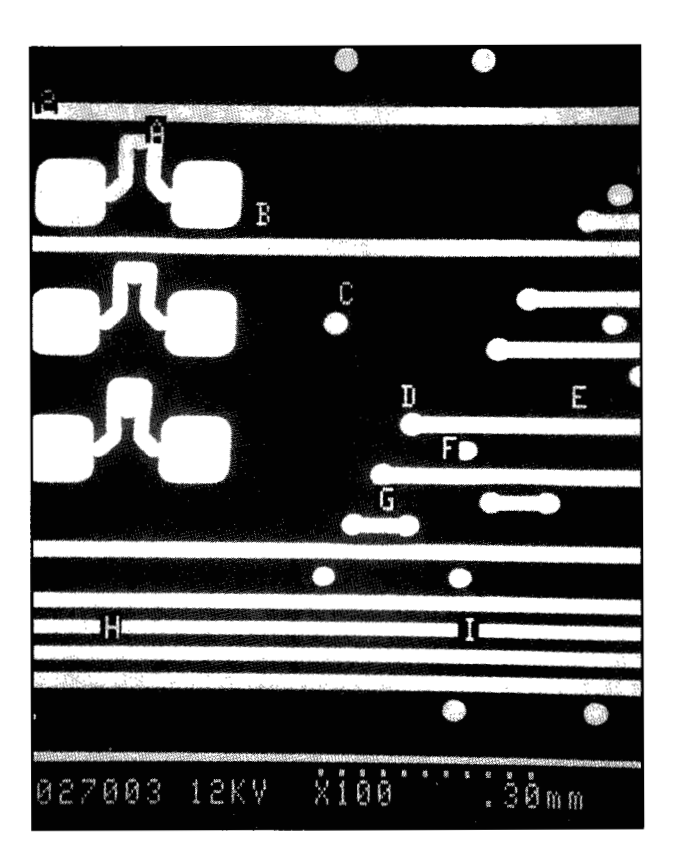
Figure 13

Graphical representation of Monte Carlo calculations of the interaction volume for X-ray generation in Co as a function of beam energy: (a) 10 keV; (b) 20 keV; (c) 30 keV.

Co layer, which is targeted to be more than an order of magnitude thinner than the Cu.

Using 10- and 12-keV beam energies, we performed thickness calibrations on samples prepared in the following way. A 2- μ m Cu layer was evaporated on silicon wafers. Cobalt dots 3.0 mm in diameter were evaporated up to different thicknesses ranging from 200 to 1750 Å, as measured by the quartz monitor and RBS. The data were plotted in the form of thickness, T_i vs. R_i , where $R = I_{Co}/I_{Cu}$ K α ; or thickness, vs. $\ln R_i$. Fitting parameters for simple polynomials were obtained with good regression values.

We use the calibration described in the previous paragraph to measure the thickness of Co(P) plated on various features in real parts. In this circumstance, because some features were electrically isolated, charging



Thicknesses (in Å) of Co(P) plated on features in a real part: A, 866; B, 678; C, 1016; D, 986; F, 804; Co, 900; H, 755; I, 735. Thicknesses of control blanket sample: 406 Å, our value; 394 Å, X-ray fluorescence (M. Sietz, private communication).

was observed. Therefore, carbon coating was necessary for charge neutralization. This may seem to be a drawback, in the sense that the proposed technique may not fall in the category of being nondestructive. However, washable conducting compounds are currently being tested for this purpose, and these sprayable materials will make the method of measurement truly nondestructive.

Figure 14 shows the results obtained in a manufactured part, with features of different sizes. Notice that the small features exhibit a much larger Co(P) thickness than the larger ones. The values obtained in this sample are very different from that obtained on the blanket control sample using X-ray fluorescence (394 Å). However, our EDX measurements recorded on the same blanket sample (average value = 406 Å) agreed with the X-ray fluorescence value. These results indicate that the Co(P) thicknesses obtained on real parts may differ from those

² M. Sietz, private communication.

predicted by plating blanket control samples for the same amount of time. Therefore, steps were taken using the described technique to ensure that all of the features in real parts were capped with electroless Co(P) satisfying a minimum specified thickness.

From the Co(P) thickness results obtained for the sample shown in Figure 14, one would expect nonlinear diffusion of the *low-concentration* ($\sim 5 \times 10^{-6}$ mol dm⁻³) Pb additive to decrease the rate of deposition at edges of large features and also at features smaller than the diffusion-layer thickness. Thus, one could expect to see thinner deposits on the smaller features, but this is not the case here. This suggests that one of the reactants in the electroless Co(P) deposition process, most likely cobalt ion, exhibits partially diffusion-controlled mass transport to the plating surface. This requires further study.

Conclusions

Electrolessly deposited materials were investigated as possible diffusion barrier layers for multilayer microelectronic substrates. Attention was focused on selectivity of deposition, barrier properties for diffusion of Cu, diffusion of barrier material into Cu (thus changing its resistivity), and the achievement of good adhesion between polyimide and the barrier layer.

- Excellent deposition selectivity was achieved by properly controlling the composition of the electroless solutions and Pd seed solution, and by addition of a complexant into the postdeposition rinse solution
- Electroless Co(P) was the most effective barrier to Cu diffusion at elevated temperature, even at Co(P) thicknesses as low as 500 Å. Electroless Ni-Co(P) and Ni(P) were less effective, but much more effective than barriers fabricated from the pure metals.
- 3. Electroless Co(P) did not interdiffuse with Cu even on extended heating at 400°C; thus, the resistivity did not change. On the other hand, Ni(P) did interdiffuse with Cu and significantly increased the resistivity of Cu under similar heating conditions.
- 4. Polyimide bonded strongly to as-deposited electroless Ni(P) layers but poorly to as-deposited Co(P). An oxidation step immediately after Co(P) film deposition that grew a passive film 50-75 Å in thickness enabled good adhesion of polyimide films to Co(P) to be reproducibly achieved.
- A low-energy-beam SEM/EDX technique was developed to measure the thickness of thin Co(P) layers. This has potential for use in connection with conductor features in other microelectronic parts.

Acknowledgments

The authors gratefully acknowledge J.-H. Kim for TEM work; R. Lacombe, P. Lauro, and J.-H. Kim for some of the early adhesion peel test measurements; M. Berger for sheet resistance measurements; and M. Komsa for sputtered seed layers. The authors wish to acknowledge useful discussions with S. Krongelb, L. Romankiw, P. Buchwalter, V. Brusic, K. McLaughlin, and many other IBM colleagues too numerous to list here.

References

- 1. A. J. Blodgett, Scientific American 249, 86 (1983).
- See, e.g., S. Kaja, S. P. Mukherjee, E. J. O'Sullivan, and M. Paunovic, U.S. Patent 5,380,560, 1995.
- 3. See IBM J. Res. Develop. 13, 226-296 (1969).
- See, e.g., N. J. Chou, D. W. Dong, J. Kim, and A. C. Liu, J. Electrochem. Soc. 131, 2335 (1984).
- J. W. Bartha, P. O. Hahn, F. Legoues, and P. S. Ho, J. Vac. Sci. Technol. A 3, 739 (1985).
- Y.-H. Kim, G. F. Walker, J. Kim, and J. Park, J. Adhes. Sci. Technol. 1, 331 (1987).
- Y.-H. Kim, J. Kim, G. F. Walker, C. Feger, and S. P. Kowalczyk, J. Adhes. Sci. Technol. 2, 95 (1988).
- G. O. Mallory and J. B. Hajdu, Eds., Electroless Plating, American Electroplaters and Surface Finishers Society, Orlando, FL, 1990.
- 9. W. Riedel, *Electroless Nickel*, ASM International, Metals Park, OH, 1991.
- J. E. A. M. van den Meerakker, J. Appl. Electrochem. 11, 395 (1981).
- M. Paunovic, P. J. Bailey, R. G. Schad, and D. A. Smith, J. Electrochem. Soc. 142, 1843 (1994).
- 12. K. Ishida and T. Nishizawa, Bull. Alloy Phase Diag. 11, 555
- 13. A. Stearn and H. Eyring, J. Phys. Chem. 44, 995 (1940).
- D. Gupta, D. R. Campbell, and P. S. Ho, in *Thin Films—Interdiffusion and Reactions*, J. M. Poate, K. N. Tu, and J. W. Mayer, Eds., John Wiley & Sons, Inc., New York, 1978, p. 161.
- 15. D. Gupta, Ibid., p. 52.
- T. Nishizawa and K. Ishida, Bull. Alloy Phase Diag. 5, 161 (1984).
- 17. D. J. Chakrabarti, D. E. Laughlin, S. W. Chen, and Y. A. Chang, *Bull. Alloy Phase Diag.* 12, 1442 (1991).
- See, e.g., R. G. Narechania, J. A. Bruce, and S. A. Fridmann, J. Electrochem. Soc. 11, 2700 (1985); J. E. Pawel and C. J. McHargue, J. Adhes. Sci. Technol. 2, 369 (1988).
- S. Kaja, E. J. O'Sullivan, and A. G. Schrott, U.S. Patents 5,382,447 and 5,453,642, 1995.
- N. S. McIntyre, D. D. Johnston, L. L. Coastworth, R. D. Davidson, and J. R. Brown, Surf. & Interface Anal. 15, 265 (1990).
- M. P. Seah, in *Practical Surface Analysis*, D. Briggs and M. P. Seah, Eds., Wiley, New York, 1983, pp. 181–216.
- 22. K. S. Kim, Phys. Rev. B 11, 3177 (1975).
- T. J. Chuang, C. R. Brundle, and D. W. Rice, Surf. Sci. 59, 413 (1976).
- 24. R. W. G. Wyckoff, *Crystal Structures*, Vol. 3, Interscience Publishers, New York, 1965, pp. 75–78.
- Handbook of Chemistry and Physics, R. C. Weast and M. J. Astle, Eds., CRC Press, Florida, 1982, p. F-182.

Received March 2, 1997; accepted for publication April 2, 1998

Eugene J. O'Sullivan IBM Research Division, Thomas J. Watson Research Center, P.O. Box 218, Yorktown Heights, New York 10598 (eosull@us.ibm.com). Dr. O'Sullivan is a Research Staff Member in the Advanced Manufacturing Technology Department. He joined the Research Division in 1984. Dr. O'Sullivan received his Ph.D. in electrochemistry from University College, Cork, Ireland, in 1981. From 1980 to 1983 he was a Postdoctoral Fellow at Case Western Reserve University, and he was a Senior Research Associate at Case from 1983 to 1984. At IBM, Dr. O'Sullivan's research has included fundamental and applied aspects of electroless metal deposition, e.g., diffusion barriers, selectivity of deposition, polyimide adhesion, and new electroless alloy deposition solutions. More recently, he has worked on the fabrication of a multilayer magnetic minimotor. Dr. O'Sullivan is currently working on aspects of MRAM device fabrication for nonvolatile memory application.

Alejandro G. Schrott IBM Research Division, Thomas J. Watson Research Center, P.O. Box 218, Yorktown Heights, New York 10598 (schrott@us.ibm.com). Dr. Schrott is a Research Staff Member in the Physical Sciences Department at the Thomas J. Watson Research Center. He did his undergraduate work at the University of Buenos Aires, Argentina, and received his Ph.D. degree in physics from the University of Washington in 1982. He subsequently worked as a Postdoctoral Associate in the Department of Materials Sciences, Cornell University. In 1984 Dr. Schrott joined the IBM Research Division, where he has worked on surface and interfacial properties of oxides and of metal-insulator systems.

Milan Paunovic IBM Research Division, Thomas J. Watson Research Center, P.O. Box 218, Yorktown Heights, New York 10598 (paunovic@us.ibm.com). Dr. Paunovic is a Research Staff Member in the Electrodeposition Technology Department at the Thomas J. Watson Research Center, working on electrochemical metal deposition for integrated circuits. He began work on electrochemical metal deposition in 1961 at the University of Pennsylvania, Philadelphia, and subsequently worked on metal deposition at Reynolds Metals, Kollmorgen, and Intel. His Ph.D. thesis at Adelphi University was on statistical mechanics of adsorption. Dr. Paunovic joined IBM in 1989. He is a coauthor of the book Fundamentals of Electrochemical Deposition, has edited four symposia proceedings volumes of the Electrochemical Society, published 41 papers, and holds seven patents.

Carlos J. Sambucetti IBM Research Division, Thomas J. Watson Research Center, P.O. Box 218, Yorktown Heights, New York 10598 (xsambuc@us.ibm.com). Dr. Sambucetti graduated from the University of Buenos Aires and the University of Minnesota and published from his thesis work a number of papers on the voltammetric behavior of solid microelectrodes. In 1972 he joined the IBM Research Division, where he received an IBM Outstanding Contribution Award for the development of new colloidal magnetic fluids. In 1980 he designed electrochemical systems to elucidate the mechanism of insulation resistance in printed-circuit boards, for which he received another IBM Outstanding Contribution Award. In 1984 he introduced in Endicott and IBM Germany a new process to enhance the catalytic activity of nonconducting films for electroless plating, for which he received an IBM Corporate Award. At the end of a two-year assignment in Sindelfingen, he was appointed in 1986 a member of the

Corporate Technical Committee in Armonk. Dr. Sambucetti was appointed an STSM and Member of the IBM Academy of Technology in 1992; he is active in the field of electroless plating applied to semiconductor technology and packaging and is the recipient of 20 invention awards.

Jeffrey R. Marino FED Corporation, Hudson Valley Research Park, 1580 Route 52, Hopewell Junction, New York 12533 (fedcorp@aol.com). Mr. Marino is currently a Microstructures Process Engineer with the FED Corporation, responsible for wet process, photolithography, and other aspects of flat-panel video display production. He received a B.A. degree in chemistry from Manhattanville College in 1992. He subsequently joined IBM at the Thomas J. Watson Research Center, where he worked with electroless and electrolytic plating as well as conductive adhesives, polymer processing, and interconnect technology.

Philip J. Bailey (deceased)

Suryanarayana Kaja IBM Microelectronics Division, East Fishkill facility, Route 52, Hopewell Junction, New York 12533 (kaja@us.ibm.com). Dr. Kaja received a Ph.D. degree in materials science and engineering from Penn State University in 1985 and joined IBM in 1989. He has been working in the field of electroplating and electroless plating of different metals and alloys for more than 15 years. He is currently responsible for developing plating processes for thin-film metallization of electronic components at the Microelectronics Division site in East Fishkill, New York. Dr. Kaja has published several papers and holds a number of patents in areas related to thin-film processing.

Krystyna W. Semkow IBM Microelectronics Division, East Fishkill facility, Route 52, Hopewell Junction, New York 12533 (ksemkow@us.ibm.com). Dr. Semkow is an Advisory Engineer in the Product Development group at the East Fishkill facility. She joined IBM at the Endicott facility in 1988. She received an M.S. degree in 1974 from Warsaw University and a Ph.D. degree in 1984 from Washington University, both in chemistry/electrochemistry. She works on plating and etching processes for thin-film and ceramic semiconductor packaging. Dr. Semkow is a member of the Electrochemical Society.